$\Delta\varepsilon t = 0.4\varepsilon_0 a$, where a = cylinder radius = 0.1016 m. Note that the principal effect of the dielectric cylinder is to shift the resonance to a lower frequency.

VII. Discussion

The impedance sheet approximation for thin dielectric shells has been used to compute the electromagnetic behavior of thin shells using computer programs developed for loaded bodies. Far-field quantities, such as radar cross section and antenna gain patterns, are probably accurate. It is expected that near-field quantities would be less accurate. The method could be extended to include the normal component of polarization current, in which case it would, in principle, be exact. However, this would complicate the solution and require the development of new computer programs.

References

[1] R. F. Harrington and J. R. Mautz, "Radiation and scattering from loaded bodies of revolution," *Appl. Sci. Res.*, vol. 26, pp. 209–217, June 1971.

[2] ——, "Computation of radiation and scattering from loaded bodies of revolution," Sci. Rep. 4, Contract F19628-68-C-0180 with Air Force Cambridge Research Laboratories, AD 701-744, Jan. 1970.

[3] ——, "Control of radar scattering by reactive loading," *IEEE Trans. Antennas Propagat.*, vol. AP-20, pp. 446–454, July 1972.

[4] M. G. Andreasen, "Backscattering cross section of a thin, dielectric, spherical shell," *IRE Trans. Antennas Progapat.*, vol. AP-5, pp. 267–270, July 1957.

[5] J. R. Wait, "Propagation of electromagnetic waves along a thin plasma sheet," *Can. J. Phys.*, vol. 28, no. 12, pp. 1586–1594, Dec. 1960.

[6] R. L. Fante, "Effect of thin plasmas on an aperture antenna in an infinite conducting plane," *Radio Sci.*, vol. 2 (new series), pp. 87–100, Jan. 1967.

[7] J. H. Richmond, "Scattering by a dielectric cylinder of arbitrary cross section shape," *IEEE Trans. Antennas Propagat.*, vol. AP-13, pp. 334–341, May 1965.

[8] R. F. Harrington, *Field Computation by Moment Methods*. New York: Macmillan, 1968.

[9] G. T. Ruck, D. E. Barrick, W. D. Stuart, and C. K. Krichbaum, *Radar Cross Section Handbook*, vol. 1. New York: Plenum, 1970.

[10] D. C. Kuo, H. H. Chao, J. R. Mautz, B. J. Strait, and R. F. Harrington, "Analysis of radiation and scattering by arbitrary configurations of thin wires," *IEEE Trans. Antennas Propagat.* (CPD), vol. AP-20, pp. 814–815, Nov. 1972.

[11] J. R. Mautz, "Scattering from loaded wire objects near a loaded surface of revolution," Syracuse University Research Corporation, Rep. SURC TN 74-030, Jan. 1974.

Analysis of Various Numerical Techniques Applied to Thin-Wire Scatterers

CHALMERS M. BUTLER AND D. R. WILTON

***Abstract*—Several numerical schemes for solving Pocklington's and Hallén's equations for thin-wire scatterers are investigated. Convergence rates of solutions obtained from seven methods are given and reasons for different rates are delineated.**

Introduction

In moment method solutions of antenna and scattering problems associated with thin-wire structures, both Pocklington (electric field) and Hallén (magnetic vector potential) type integral equations are commonly used. From either, one may obtain solutions for the current on a wire antenna or a scatterer and subsequently calculate all other quantities of interest. Even though the two equations are intimately related [1], each exhibits distinct advantages and disadvantages. The authors present the findings of their investigations of several numerical schemes for solving wire problems. They discuss the relative merits of various techniques, point out pitfalls to be avoided, and summarize their findings.

Manuscript received August 1, 1974; revised December 23, 1974. This work was supported in part by the National Science Foundation under Grant GU3833.

The authors are with the School of Engineering, University of Mississippi, University, Miss. 38677.

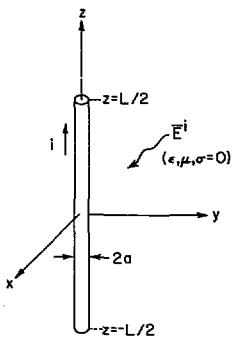

Fig. 1. Straight wire subject to incident illumination.

In the numerical methods, different basis sets for representing the unknown wire current are employed and relative convergences are investigated. So that one may focus attention on the generic feature of the capacity of a given basis set to represent adequately, and converge to, the correct current on the wire, only the case of a scatterer subject to normally incident illumination is considered here. With illumination constant over the length of the scatterer, the problem of inadequate sampling [2] of the integral equation's driving term has no bearing on convergence. Also, in the interest of simplicity and of addressing only the fundamental question of convergence in the sense of how well the actual wire current is represented by the solution, the wire junction problem is not treated nor is any record of computer times given for the various methods.

Thin-Wire Equations

From basic electromagnetic theory, one may readily obtain the following fundamental integro-differential equation:

$$\left(\frac{d^2}{dz^2} + k^2\right)\int_{\zeta=-L/2}^{L/2} i(\zeta)K(z-\zeta)\,d\zeta = -j4\pi\omega\varepsilon E_z^i(z) \quad (1)$$

which relates the unknown total axial current i on a cylinder to the known incident electric field having an axial component E_z^i on the surface of the scatterer. The scatterer is perfectly conducting and resides in a homogeneous space characterized by (μ, ε, $\sigma = 0$), and, as suggested in Fig. 1, it is a tube of length L and radius a. The kernel in (1) is

$$K(\xi) = \frac{1}{2\pi}\int_{\phi'=-\pi}^{\pi} \frac{e^{-jk[\xi^2+4a^2\sin^2(\phi'/2)]^{1/2}}}{[\xi^2 + 4a^2\sin^2(\phi'/2)]^{1/2}}\,d\phi' \quad (2)$$

where k is 2π/wavelength at the angular frequency ω of the suppressed harmonic time variation $e^{j\omega t}$. For present purposes, the wire radius is looked upon as being very small relative to the wavelength λ as well as to the cylinder length. Such restrictions, common in thin-wire analyses, assure one that the current on the cylinder is circumferentially independent and that it can be accounted for by the total axial current i. The thin-wire assumptions also lead to the so-called reduced kernel approximation to $K(\xi)$

$$K(\xi) \doteq \frac{e^{-jk[\xi^2+a^2]^{1/2}}}{[\xi^2 + a^2]^{1/2}}. \quad (3)$$

From (1), one may readily derive Hallén's equation

$$\int_{\zeta=-L/2}^{L/2} i(\zeta)K(z-\zeta)\,d\zeta = C\cos kz + B\sin kz - j\frac{4\pi}{\eta}\int_{\zeta=0}^{z} E_z^i(\zeta)\sin k(z-\zeta)\,d\zeta \quad (4)$$

where $\eta\ (=\sqrt{\mu/\varepsilon})$ is the intrinsic impedance of the medium and where C and B are constants of integration which must be consistent with the boundary condition that the current be zero at the wire ends ($\pm L/2$). In the special case of normally incident plane wave illumination, E_z^i is constant over $z \in (-L/2,L/2)$ allowing one to perform analytically the integration on the right side of (4), and $i(z)$ is an even function of z allowing one to eliminate the constant B. The exact kernel (2) may be used in (4) or, where warranted by thin-wire conditions, the approximation (3) often suffices.

Having accepted the approximation (3), one may interchange at will the integral and differential operators in (1) and, thereby, convert it to any of several equivalent forms usually referred to as Pocklington-type equations. For the present discussion, the form which is most useful is

$$\int_{\zeta=-L/2}^{L/2}\left[\left(\frac{d^2}{d\zeta^2}+k^2\right)i(\zeta)\right]K(z-\zeta)\,d\zeta + \left[i(\zeta)\frac{\partial}{\partial\zeta}K(z-\zeta) - \frac{d}{d\zeta}i(\zeta)K(z-\zeta)\right]_{\zeta=-L/2}^{L/2} = -j4\pi\omega\varepsilon E_z^i(z). \quad (5)$$

Bases

The unknown current $i(z)$ is represented in a numerical solution technique by a linear combination of known elements $i_n(z)$ of a basis set $\{i_n(z)\}$ selected to approximate the current as

$$i(z) \doteq \sum_n I_n i_n(z). \quad (6)$$

With i in the integral equations replaced by its approximation of (6), Hallén's and Pocklington's equations become, respectively,

$$\sum_n I_n \int_{\zeta=l_n}^{u_n} i_n(\zeta)K(z-\zeta)\,d\zeta = C\cos kz + B\sin kz - j\frac{4\pi}{\eta}\int_{\zeta=0}^{z} E_z^i(\zeta)\sin k(z-\zeta)\,d\zeta \quad (7a)$$

and

$$\sum_n I_n\left\{\int_{\zeta=l_n}^{u_n}\left[\left(\frac{d^2}{d\zeta^2}+k^2\right)i_n(\zeta)\right]K(z-\zeta)\,d\zeta + \left[i_n(\zeta)\frac{\partial}{\partial\xi}K(z-\zeta) - \frac{d}{d\zeta}i_n(\zeta)K(z-\zeta)\right]_{\zeta=l_n}^{u_n}\right\} = -j4\pi\omega\varepsilon E_z^i(z). \quad (7b)$$

One chooses the set $\{i_n\}$ for its capacity to represent the current well and from the viewpoint of its utility in the numerical procedure. The basis sets considered here are illustrated in Fig. 2 and are defined subsequently where one sees them to be of the subdomain type, since each element i_n differs from zero over only a single subdomain of the total domain of interest $z \in (-L/2,L/2)$.

Piecewise Sinusoidal:

$$i_n(z) = \begin{cases}\dfrac{\sin k(\Delta - |z-z_n|)}{\sin k\Delta}, & z \in (z_{n-1},z_{n+1}) \\ 0, & z \notin (z_{n-1},z_{n+1})\end{cases} \quad (8a)$$

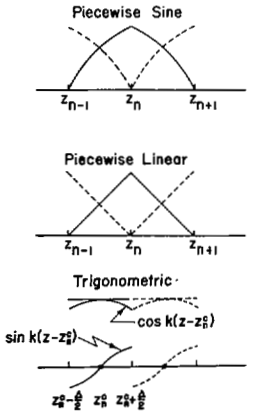

Fig. 2. Bases.

Piecewise Linear:

$$i_n(z) = \begin{cases}\dfrac{\Delta - |z-z_n|}{\Delta}, & z \in (z_{n-1},z_{n+1}) \\ 0, & z \notin (z_{n-1},z_{n+1})\end{cases} \quad (8b)$$

Trigonometric:

$$i_n(z) = \begin{cases}1 + C_n\cos k(z-z_n^c) + B_n\sin k(z-z_n^c), \\ \qquad z \in (z_n^c - \Delta/2,\ z_n^c + \Delta/2) \\ 0, \qquad z \notin (z_n^c - \Delta/2,\ z_n^c + \Delta/2).\end{cases} \quad (8c)$$

Entire domain basis sets where each element exists over the full domain $(-L/2,L/2)$ are useful in special cases, but, since their application is limited, they are not treated in this paper.

Implicit in the use of (8) in (7) is the division of the scatterer length L into N subintervals of length $\Delta = L/N$. In all cases the boundary conditions $i(\pm L/2) = 0$ are satisfied by (6) *a priori* which, in using (8a) and (8b), means that one sets the I_n associated with the i_n over the intervals $(L/2 - \Delta, L/2 + \Delta)$ and $(-L/2 - \Delta, -L/2 + \Delta)$ equal to zero whereas with (8c) the C_n and B_n of the end-most intervals are adjusted so that $i(\pm L/2) = 0$. For piecewise linear and piecewise sinusoidal basis sets, the interval (l_n,u_n) must be partitioned into (z_{n-1},z_n) plus (z_n,z_{n+1}) and the terms on the left side of (7b) must be evaluated in each of these two open intervals and summed to obtain the contribution from (l_n,u_n). This partitioning is necessary due to the derivative discontinuity at z_n exhibited by both (8a) and (8b). For the trigonometric set, $l_n = z_n^c - \Delta/2$ and $u_n = z_n^c + \Delta/2$, where z_n^c is the center of the nth subdomain.

As discussed in detail subsequently, the convergence rate of a solution method can be enhanced by modification of (6) through certain constraints applied to $\{i_n\}$. Two such constraints are employed by the authors in methods discussed forthwith. In one case they adjust the C_n and B_n of (8c) to force i of (6) plus its derivative to be continuous at each common boundary point of adjacent subdomains. Subject to these adjustments of the coefficients in (8c), a basis set is obtained which renders the current and its first derivative continuous everywhere in $(-L/2,L/2)$. In another case employing (8c), $i_n(z)$, the current in the nth subdomain, is required to satisfy[1] $i_n(z_{n-1}^c) = i_{n-1}(z_{n-1}^c)$ and $i_n(z_{n+1}^c) = i_{n+1}(z_{n+1}^c)$. One might refer to this as *extrapolated continuity*, and it is evident that the requirements do not force the current or its derivative to be continuous at the boundary of subdomains.

[1] See [3].

Testing

Substitution of (6) into (4) and (5) yields (7a) and (7b), respectively, in which all integrations and differentiations operate on known functions but into which the additional unknown constants I_n are introduced.

According to the method of moments [4], one can transform (7a) or (7b) into a system of linear algebraic equations with unknowns I_n by testing both sides of either equation with members of a suitable testing set $\{W_m\}$. For example, testing of (7b) yields

$$\sum_n I_n \left\langle \int_{\zeta=l_n}^{u_n} \left[\left(\frac{d^2}{d\zeta^2} + k^2 \right) i_n(\zeta) \right] K(z-\zeta)\, d\zeta + \left[i_n(\zeta) \frac{\partial}{\partial \zeta} K(z-\zeta) - \frac{d}{d\zeta} i_n(\zeta) K(z-\zeta) \right]_{\zeta=l_n}^{u_n}, W_m(z) \right\rangle = -j4\pi\omega\varepsilon \langle E_z^i(z), W_m(z) \rangle, \quad m = 1,2,\cdots,M \tag{9}$$

where

$$\langle f, W \rangle = \int_{z=-L/2}^{L/2} f(z) W(z)\, dz.$$

In the preceding (9) is a system of linear equations which can be solved for the I_n for proper M.

Discussion of Methods

In this section the seven solution methods in Table I are discussed in the order of their listing, and relative convergence data are given in Figs. 3–12. The value of current at the center of the scatterer is the quantity upon which the study of convergence is based, since it was ascertained that the convergence rate at points other than the scatterer center was comparable to that of the center current. In all cases, data are normalized with respect to that obtained from Galerkin's method with 31 piecewise sinusoids. Normalized results of each method are plotted against $1/N$ where one recalls N to be the total number of subdomains into which $(-L/2,L/2)$ is divided. In Methods I, II, III, and VI the number of unknown I_n to be determined is $(N-1)$, while in Method V the number of unknown current coefficients is N. After constraining the C_n and B_n of (8c) in Method IV, one has N unknown I_n to calculate but these constraining equations either augment the system of equations (9) or necessitate that one solve an auxiliary difference equation. Finally, the number of unknown I_n in Method VII is $(N-1)$ but the two constants C and B are unknown *a priori* so that, effectively, one must solve for $N+1$ quantities.

Data are given for two radii and for selected wire lengths so that they include special cases of practical interest, e.g., $L = \lambda/2$ and $L = \lambda$. Trends inferred from data given should be representative of typical cases encountered in practice except, of course, for very long wires.

The real and imaginary parts of the center current are investigated separately and each part is normalized with respect to the corresponding part obtained from Galerkin's method as mentioned. The real and imaginary normalization factors, C_R and C_I, are given in each figure. Normalization of each part separately has the advantage that small differences in a part can be independently observed in the data. However, on the other hand, when C_R and C_I differ appreciably, deviations from the norm of data normalized with respect to the smaller may be in large measure due to round-off errors; such a deviation appears extreme to an observer when actually it is of no consequence upon comparison with $\sqrt{C_R^2 + C_I^2}$.

TABLE I
Numerical Solution Methods

Method	Equation	Basis Set	Testing Method	Key
I	Pocklington	Piecewise sinusoidal	Collocation	P-PS-C
II	Pocklington	Piecewise sinusoidal	Collocation/ Galerkin	P-PS-C/G
III	Pocklington	Piecewise sinusoidal	Galerkin	P-PS-G
IV	Pocklington	Trigonometric with continuous current and continuous derivative	Collocation	P-T/C-C
V	Pocklington	Trigonometric with extrapolated continuity	Collocation	P-T/E-C
VI	Pocklington (Difference Equation)	Piecewise linear	Collocation	P-PL-DE
VII	Hallén	Piecewise linear	Collocation	H-PL-C

Method I (Pocklington-Piecewise Sinusoid-Collocation)

Since no numerical integration is needed to calculate terms in (9), Pocklington's equation subject to collocation $(W_m(z) = \delta(z - z_m))$ with the piecewise sinusoids (8a) in the current approximation (6) appears, superficially, to be a very attractive method. No numerical integration is needed in (9), since the harmonic differential operator in the integrand applied to (8a) yields zero for $\zeta \in (z_n, z_{n+1})$, leaving one with simply

$$\frac{k}{\sin k\Delta} \sum_n I_n [K(z_m - z_{n-1}) - 2\cos k\Delta K(z_m - z_n) + K(z_m - z_{n+1})] = -j4\pi\omega\varepsilon E_z^i(z_m)$$

where $z_m = m\Delta$, $m = 0, \pm 1, \pm 2, \cdots, \pm(N-2)/2$, are the match points in $(-L/2,L/2)$ at which (9) is enforced. Unfortunately, the obviation of numerical integration not withstanding, this procedure is unsatisfactory except for large radius and/or resonant length wires. Under close scrutiny the method is not generally satisfactory even for a large radius wire, since the solution converges rapidly for relatively small N, but with further increase in N the system of linear equations (9) which one must solve to determine the coefficients I_n becomes ill-conditioned [5]. These comments are supported by the data of Figs. 3–12 where one sees that for $a = 0.01\lambda$ the method enjoys somewhat better convergence than for $a = 0.001\lambda$ except when $L = 0.5\lambda$; also, P-PS-C exhibits better convergence for $L = 0.5\lambda$ and $a = 0.001\lambda$ than for other lengths and this radius.

Method II (Pocklington-Piecewise Sinusoid-Collocation/ Galerkin)

Initially the authors attributed the poor convergence of P-PS-C to the fact that the integral equation is enforced at the interior points (match points z_m) but not at the end points $(\pm L/2)$ with the consequence that the resulting system (9) may characterize a scatterer of length $L - 2\Delta$ rather than of L, the correct value. As a remedy, they elected to form (9) by testing over $(-L/2, -L/2 + 2\Delta)$ and $(L/2 - 2\Delta, L/2)$ with the piecewise sinusoids of (8a) and point-matching at the interior points (match points z_m). This hybrid testing procedure (Method II) is designated P-PS-C/G. Deceptively, it appears to converge for small N but is little better than P-PS-C for larger N as is seen from the data of Figs. 3–12.

Further investigation of (8) and (9) reveals that the poor convergence rates of P-PS-C and P-PS-C/G are due to the rapidly

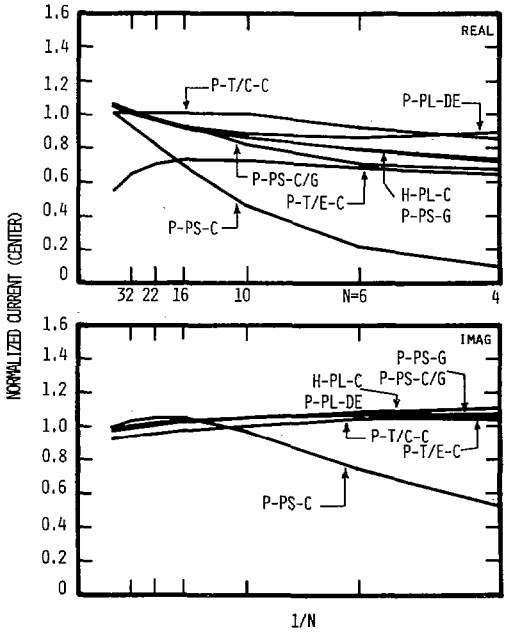

Fig. 3. Convergence data: normalized current at center of scatterer versus 1/number of subdomains ($l = 0.4\lambda$, $a = 0.01\lambda$, $C_R = 3.007$, $C_I = 2.310$).

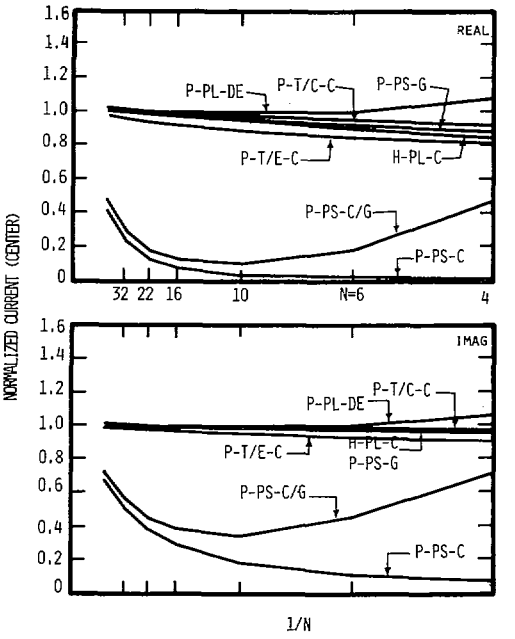

Fig. 4. Convergence data: normalized current at center of scatterer versus 1/number of subdomains ($l = 0.4\lambda$, $a = 0.001\lambda$, $C_R = 0.5498$, $C_I = 1.566$).

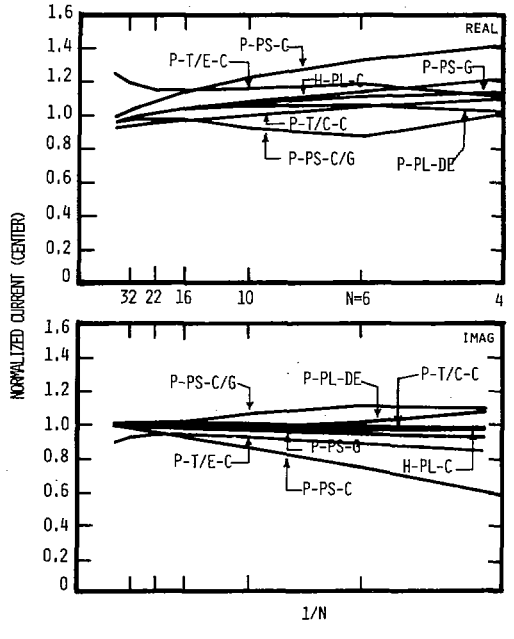

Fig. 5. Convergence data: normalized current at center of scatterer versus 1/number of subdomains ($l = 0.5\lambda$, $a = 0.01\lambda$, $C_R = 2.808$, $C_I = -0.908$).

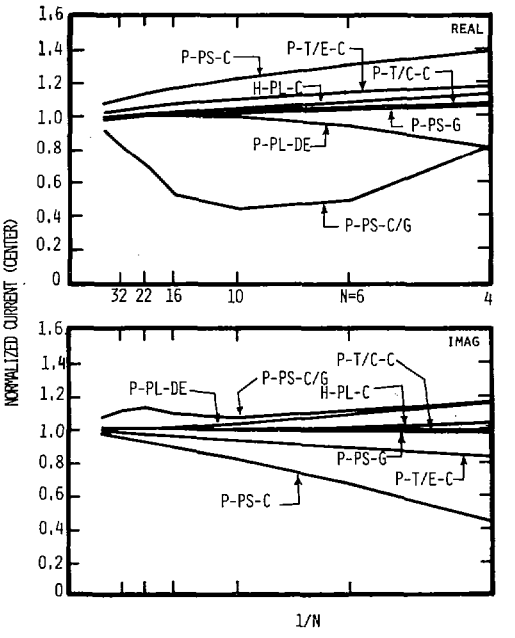

Fig. 6. Convergence data: normalized current at center of scatterer versus 1/number of subdomains ($l = 0.5\lambda$, $a = 0.001\lambda$, $C_R = 2.999$, $C_I = -1.929$).

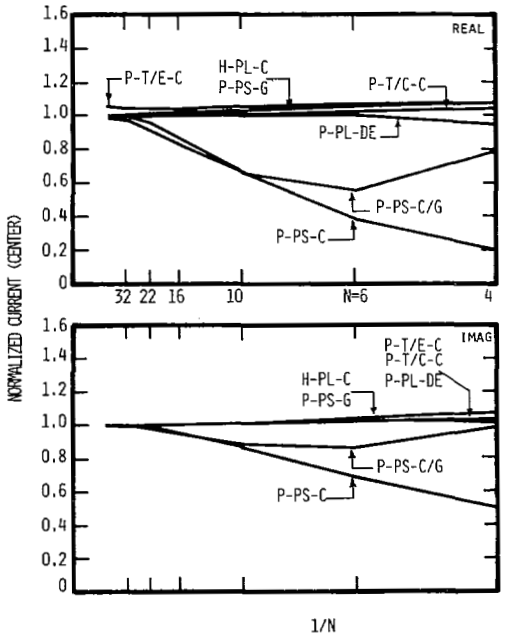

Fig. 7. Convergence data: normalized current at center of scatterer versus 1/number of subdomains ($l = 0.667\lambda$, $a = 0.01\lambda$, $C_R = 1.038$, $C_I = -1.619$).

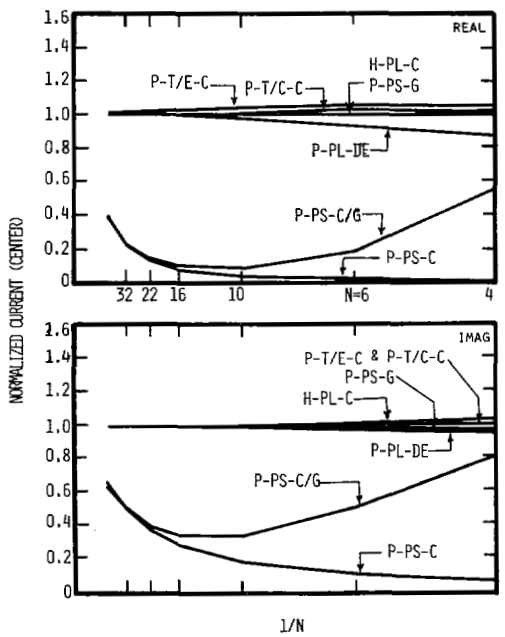

Fig. 8. Convergence data: normalized current at center of scatterer versus 1/number of subdomains ($l = 0.667\lambda$, $a = 0.001\lambda$, $C_R = 0.4658$, $C_I = -1.210$).

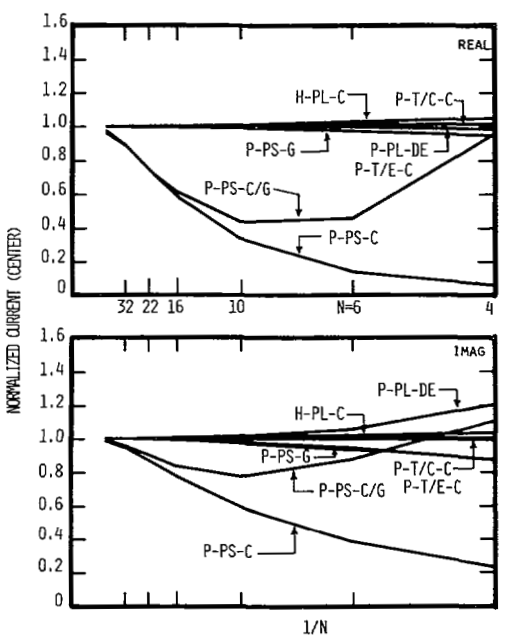

Fig. 9. Convergence data: normalized current at center of scatterer versus 1/number of subdomains ($l = 1.\lambda$, $a = 0.01\lambda$, $C_R = 0.6482$, $C_I = -1.450$).

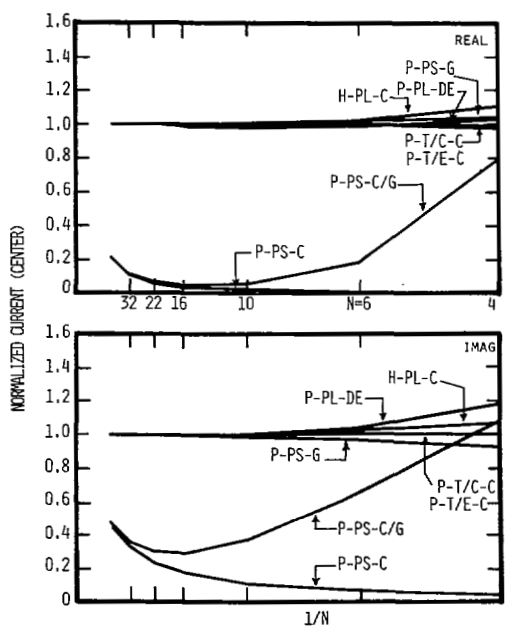

Fig. 10. Convergence data: normalized current at center of scatterer versus 1/number of subdomains ($l = 1.\lambda$, $a = 0.001\lambda$, $C_R = 0.2479$, $C_I = -0.9328$).

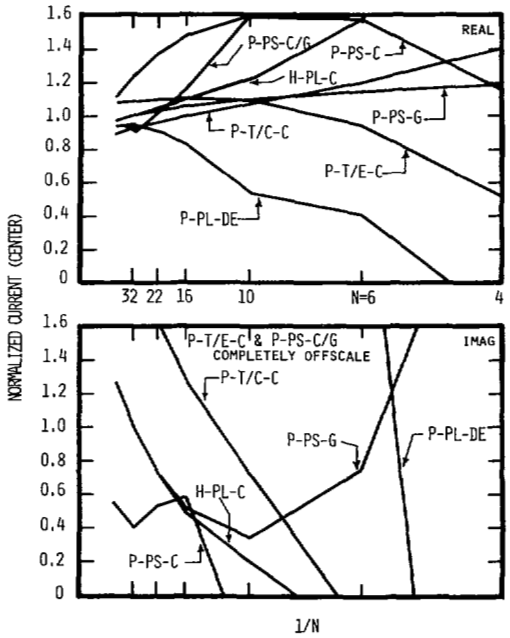

Fig. 11. Convergence data: normalized current at center of scatterer versus 1/number of subdomains ($l = 1.5\lambda$, $a = 0.01\lambda$, $C_R = -1.711$, $C_I = 0.0788$).

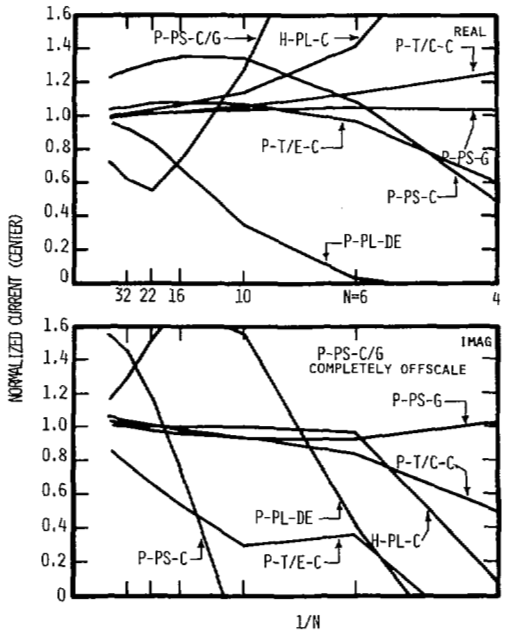

Fig. 12. Convergence data: normalized current at center of scatterer versus 1/number of subdomains ($l = 1.5\lambda$, $a = 0.001\lambda$, $C_R = -2.175$, $C_I = 0.4404$).

varying contributions to the scattered electric field arising from the unnatural discontinuities in derivative of the current approximation formed from the piecewise sinusoidal basis set [2]. Notice, however, in Figs. 5 and 6, the acceptable convergence rates of P-PS-C for resonant-length elements, which are due to the fact that resonant current is almost sinusoidal and the discontinuities in derivative almost vanish [1], [2].

A discontinuity in current or its derivative is unphysical and any approximation (6) exhibiting either produces a rapidly varying scattered electric field [2]. In particular, at a discontinuity in current, there is a contribution to scattered field proportional to $(\partial/\partial\zeta)K(z - \zeta)_{z=\zeta}$ as is seen from (5), whereas at a discontinuity of derivative of current there is a contribution proportional to $K(0)$. With either discontinuity, a highly peaked, rapidly varying scattered electric field is produced along the scatterer, which according to (5) must be equal to the constant $-E_z^i$ (normal incidence). Of course, equating of a constant to a rapidly varying function at discrete points z_m is unlikely to give rise to equality at points other than z_m over the interval $(-L/2, L/2)$.

Method III (Pocklington-Piecewise Sinusoid-Galerkin)

Failure to satisfy (7b) in some sense at all points on the scatterer implies, of course, a poor solution and, in P-PS-C and P-PS-C/G, can be attributed to the unnatural variation of the scattered electric field caused by unphysical discontinuities in the derivative of (6), the representation of current. In an attempt to improve solution methods employing basis sets which introduce discontinuities in the approximation to the current or its derivative, one may equate weighted averages of both sides of (7b) in hopes of achieving a better representation of the scattered field over the entire range $(-L/2, L/2)$ compared with its values at discrete z_m. Galerkin's method, which is mentioned under TESTING, effects such averaging. P-PS-G is a technique for solving Pocklington's equation by Galerkin's method with piecewise sinusoids both for representing the current and for testing. Solutions obtained by means of P-PS-G are seen from Figs. 3–12 to converge rapidly. Note that the Galerkin procedure requires two integrations, one over the basis element and another over the testing function. Richmond, who calls this procedure "piecewise sinusoidal reaction matching," has shown, however, that these integrations can be performed analytically for piecewise sinusoidal basis and testing sets [6], [1].

Notice that Methods I, II, and III incorporate (8a) in (6), each with different testing schemes for solving Pocklington's equation. Since, for $\Delta \ll \lambda$, (8b) closely approximates (8a), comments for the piecewise sinusoid also hold for the piecewise linear basis set.

Method IV (Pocklington-Trigonometric/Continuous Current and Derivative-Collocation)

In keeping with the desire to maintain continuity of current and its derivative over the scatterer, the authors investigated the use of the trigonometric set (8c) in Pocklington's equation, but, in addition to point-matching at the center of each subdomain, i and $(di/d\zeta)$ were forced to be equal at the common boundary points of adjacent subdomains.[2] Note that such a current representation may be called a trigonometric spline function. Solutions obtained by this method P-T/C-C are seen to converge rapidly (Figs. 3–12) as one would expect.

Method V (Pocklington-Trigonometric/Extrapolated Continuity-Collocation)

Because the introduction in P-T/C-C of the equations to maintain continuity of (6) and its derivative adds significant complexity to the method, an alternate scheme, P-T/E-C, for suppressing the discontinuities was investigated. Subject to *extrapolated continuity*[3] of P-T/E-C, the discontinuities are not zero but are reduced to levels at which their contributions do not dominate the scattered field. In contrast to the unacceptable

[2] See last paragraph under BASES.
[3] See last paragraph under BASES and [3].

complexities encountered in P-T/C-C in constraining the C_n and B_n, P-T/E-C is not difficult to implement, yet one observes from Figs. 3–12 that the convergence rate of solutions obtained by the latter method is near that of those obtained by the former. However, for larger and larger N, P-T/E-C solutions are seen to exhibit trends of diverging. This divergence is understandable, since in P-T/E-C the discontinuities are not zero, and, as $\Delta \to 0$ for larger and larger N, the unnatural contributions due to $K(\Delta/2)$ and $(\partial/\partial\zeta)K(z-\zeta)_{z-\zeta=\Delta/2}$ become more and more significant.

Modifications of P-T/E-C and P-T/C-C where the trigonometric functions of (8c) are replaced by other analytic functions, e.g., three-term power series, also lead to satisfactory solution techniques.

Method VI (Pocklington-Piecewise Linear-Difference Equation)

Methods I–V exhibit convergence rates which strongly depend upon how one handles discontinuities of (6) and its derivative. As an alternative to placing continuity requirements upon (6) to suppress the peaked field variations, one may relax or smooth the derivatives in (1) that operate on

$$\int_{\zeta=-L/2}^{L/2} i(\zeta)K(z-\zeta)\,d\zeta \tag{10}$$

to produce these unnatural contributions to scattered electric field at the discontinuities. In particular in P-PL-DE the harmonic operator of (1) may be replaced by its corresponding difference operator; the difference operator is insensitive to the local variation of (10) due to discontinuities of (6) but does correctly account for desired global derivatives. Specifically, in P-PL-DE, the derivative discontinuities of the piecewise linear representation, (8b) in (6), do not manifest themselves in sharp peaks of the scattered field. Moreover, the difference operator equation approximation to (1) is amenable to use with basis sets which cause discontinuities in (6) as well as in its derivative. The convergence of P-PL-DE is given in Figs. 3–12 [1].

Method VII (Hallén-Piecewise Linear-Collocation)

Pocklington's equation relates the electric field to the sources on the scatterer in such a manner that the value of field is very sensitive to both the current and its derivative and, consequently, any efficient method for solving this equation must include special treatment of either the derivatives or of the discontinuities. On the other hand, Hallén's equation is based on the vector potential and the electric field enters the relationship only through integration. In addition, the vector potential is less sensitive to local variation of current than is its second derivative so Hallén's equation yields to solution methods in which the current is approximated (6) by unphysical currents possessing discontinuities. Good convergence is seen in solutions of Hallén's equation when the basis set is piecewise linear (H-PL-C) and in which no attempt is made to lessen the effects of the discontinuous derivatives (Figs. 3–12).

Conclusions

Seven methods for determining the current on a scatterer are presented and the relative convergence rates of the solutions obtained by the methods are investigated. Reasons for differences in rates are delineated. It is shown that, if acceptable convergence rates are to be attained, solution methods applied to Pocklington's equation must incorporate means of suppressing discontinuities in the current approximation and its derivative, or, on the other hand, the deleterious effects of these discontinuities must be circumvented by rendering the equation insensitive to them. The latter can be accomplished by averaging techniques applied to both sides of the equation, e.g., Galerkin's method, or by smoothing the derivatives, e.g., use of difference operator. Hallén's equation governs quantities which are less sensitive to discontinuities and it may be successfully solved numerically with almost any reasonable basis set, even one which causes the approximate current to be discontinuous. For a given basis set, the convergence rate of solutions to Hallén's equation obtained by point-matching is as high as that of solutions to Pocklington's equation with any testing scheme. Solutions by the difference equation method attain a high rate of convergence essentially identical to that of the point-matched Hallén equation. Of further importance, the difference equation procedure is simple, and it is highly amenable to numerical implementation, even when applied to multiple-wire structures.

References

[1] D. R. Wilton and C. M. Butler, "Use of difference equations in conjunction with moment methods," in *USNC/URSI 1974 Spring Meeting*, Atlanta, Ga., June 1974.
[2] L. W. Pearson and C. M. Butler, "Inadequacies of collocation solutions to Pocklington-type models of thin-wire structures," *IEEE Trans. Antennas Propagat.* (Commun.), vol. AP-23, pp. 295–298, Mar. 1975.
[3] Y. S. Yeh and K. K. Mei, "Theory of conical equiangular-spiral antennas, Part I—numerical technique," *IEEE Trans. Antennas Propagat.*, vol. AP-15, pp. 634–639, Sept. 1967.
[4] R. F. Harrington, *Field Computation by Moment Methods*. New York: Macmillan, 1968.
[5] C. D. Taylor and D. R. Wilton, "The extended boundary condition solution of the dipole antenna of revolution," *IEEE Trans. Antennas Propagat.* (Commun.), vol. AP-20, pp. 772–776, Nov. 1972.
[6] J. H. Richmond and N. H. Geary, "Mutual impedance between coplanar-skew dipoles," *IEEE Trans. Antennas Propagat.* (Commun.), vol. AP-18, pp. 414–416, May 1970.

The Singularity Expansion Method as Applied to Perpendicular Crossed Wires

TERRY T. CROW, BILLY D. GRAVES, AND CLAYBORNE D. TAYLOR

***Abstract*—The singularity expansion method (SEM) has been applied to determine the current and charge induced on a system of perpendicular crossed cylinders. The SEM characteristics of this structure have been studied as the various parameters are varied. The time domain response of one particular geometry has been obtained by SEM and compared to that determined by the more conventional frequency domain analysis and Fourier inversion.**

I. Introduction

The singularity expansion method (SEM) as first discussed by Baum [1] has been elaborated and applied in a series of recent papers [2]–[5]. Using SEM it is possible to determine the time domain scattering from a conducting object in terms of a summation of damped sinusoids. This technique appears to be particularly advantageous in treating scattering from wire configurations that may be useful to model complex physical structures such as aircraft. In this report SEM is applied to determine the current and charge induced on a system of two perpendicular crossed thin cylinders (wires) in free space. This configuration may be viewed as a crude model of an aircraft. The induced current and charge are obtained as various parameters of the problem are varied.

Manuscript received June 24, 1974; revised October 31, 1974.
The authors are with the Department of Electrical Engineering, Mississippi State University, State College, Miss. 39762.